Self-Commissioning for Surface-Mounted Permanent Magnet Synchronous Motors

Naomitsu Urasaki, Tomonobu Senjyu, and Katsumi Uezato
University of the Ryukyus
1 Senbaru Nishihara-cho Nakagami Okinawa 903-0213, Japan

Abstract - This paper presents the self-commissioning for surface-mounted permanent magnet synchronous motor. The proposed strategy executes three tests with a standard inverter drive system. To do this, synchronous d-q axes currents are appropriately controlled for each test. From the three tests, armature resistance, armature inductance, equivalent iron loss resistance, and emf coefficient are identified automatically. The validity of the proposed strategy is confirmed by experimental results.

I. Introduction

Recently, sensorless control, high efficiency control, flux weakening control, and iron loss compensation control for inverter fed vector controlled surface-permanent magnet synchronous motor (SPMSM) drive have widely been developed. These control methods strongly depend on the electrical parameters. Then, these parameters should be identified in advance. However, it spends much time and energy trying to identify parameters by manual operations. An inverter with self-commissioning solves the problems. For this reason, self-commissioning strategies have been attracted attention [1][2].

This paper proposes a self-commissioning for SPMSM. The proposed self-commissioning consists of three tests, *i.e.*, dc test, single-phase ac test, and synchronous drive test. To automatically realize these test with using ordinary inverter system, synchronous d-q axes currents are appropriately controlled for each test. Since the proposed method identifies all the electrical parameters in standstill except for the emf constant, the implementation is simple. Furthermore• the iron loss resistance can also be identified. Then, the proposed method is suitable for the vector control strategies considering iron loss. The automatic identification results are experimentally compared with the measurement results by manual operations.

II. Formulation of SPMSM Taking Iron Loss Into Account

In the synchronous reference frame (d-q axes), the voltage equation for SPMSM is expressed as

$$\left.\begin{aligned} v_d &= Ri_d + p\Psi_d - \omega_r\Psi_q \\ v_q &= Ri_q + p\Psi_q + \omega_r\Psi_d \end{aligned}\right\} \quad (1)$$

where v_{dq}, i_{dq}, and Ψ_{dq} are the d-q axes stator voltages, currents, and flux linkages, respectively, R, ω_r, and p are the armature resistance, rotor speed, and differential operator, respectively. The stator flux linkages are expressed as

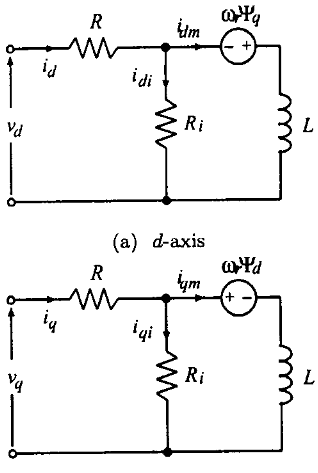

Fig. 1. d-q axes equivalent circuit for SPMSM.

$$\left.\begin{aligned} \Psi_d &= Li_{dm} + K_e \\ \Psi_q &= Li_{qm} \end{aligned}\right\} \quad (2)$$

where L and K_e are the armature inductance and emf constant, respectively. The d-q axes equivalent circuit for SPMSM is shown in Fig. 1.

III. Self-Commissioning Strategy

The automatic identifications of electrical parameters of SPMSM are implemented from a series of individual test. These tests contain the dc test, single-phase ac test, and synchronous drive test.

A. DC Test

The the dc test topology is shown in Fig. 2. When a dc voltage is applied, the SPMSM stop at the rotor speed $\theta_r = 0$ (ω_r=0). In this case, the relationship between the applied dc current/voltage and the phase current/voltage becomes as follows:

$$\left.\begin{aligned} &i_a = I_{DC}, \quad i_b = i_c = -\frac{1}{2}I_{DC} \\ &v_a = \frac{2}{3}V_{DC}, \quad v_b = v_c = -\frac{1}{3}V_{DC} \end{aligned}\right\}. \quad (3)$$

Proceedings ICPE '01, Seoul

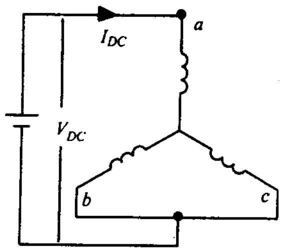

Fig. 2. DC test topology.

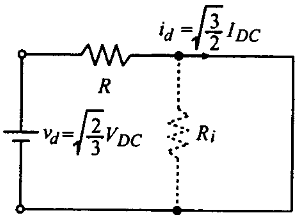

(a) *d*-axis

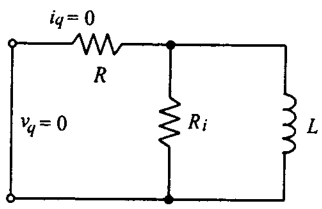

(b) *q*-axis

Fig. 3. *d*-*q* axes equivalent circuit under dc test.

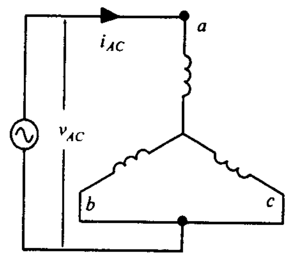

Fig. 4. Single-phase ac test topology.

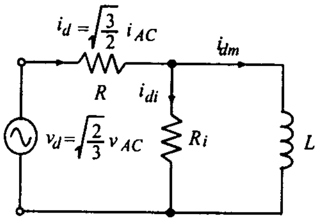

(a) *d*-axis

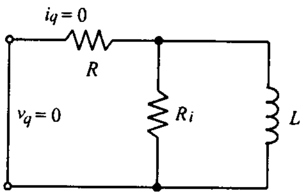

(b) *q*-axis

Fig. 5. *d*-*q* axes equivalent circuit under single-phase ac test.

Transforming the the three-phase quantities into the synchronous *d*-*q* quantities with using the transformation matrix:

$$[C]=\sqrt{\frac{2}{3}}\begin{bmatrix}\cos\theta_r & \cos(\theta_r-\frac{2}{3}\pi) & \cos(\theta_r+\frac{2}{3}\pi)\\ -\sin\theta_r & -\sin(\theta_r-\frac{2}{3}\pi) & -\sin(\theta_r+\frac{2}{3}\pi)\end{bmatrix} \quad (4)$$

we obtain the *d*-*q* axes current and voltage as

$$\left.\begin{aligned} i_d &= \sqrt{\frac{3}{2}}I_{DC}, \quad i_q = 0\\ v_d &= \sqrt{\frac{2}{3}}V_{DC}, \quad v_q = 0\end{aligned}\right\}. \quad (5)$$

Accordingly, the *d*-*q* axes equivalent circuit is reconstructed as shown in Fig. 3. It follows from Fig. 3(a) that the *d*-axis impedance $\dot{Z}_d^{DC}$ is equal to the armature resistance R. Since $\dot{Z}_d^{DC} = \dot{V}_d/\dot{I}_d$, the armature resistance is identified as

$$R=\frac{2}{3}\frac{V_{DC}}{I_{DC}}. \quad (6)$$

B. Single-Phase AC Test

The single-phase ac test topology is shown in Fig. 4. When a single-phase ac voltage is applied, the SPMSM stops at $\theta_r = 0$ ($\omega_r = 0$). In this case, the relationship between the applied ac current/voltage and phase current/voltage becomes as follows:

$$\left.\begin{aligned} i_a &= i_{AC}, \quad i_b = i_c = -\frac{1}{2}i_{AC}\\ v_a &= \frac{2}{3}v_{AC}, \quad v_b = v_c = -\frac{1}{3}v_{AC}\end{aligned}\right\}. \quad (7)$$

Transforming the three-phase quantities into the synchronous *d*-*q* quantities with using (4), we obtain the *d*-*q* axes current and voltage as

$$\left.\begin{aligned} i_d &= \sqrt{\frac{3}{2}}i_{AC}, \quad i_q = 0\\ v_d &= \sqrt{\frac{2}{3}}v_{AC}, \quad v_q = 0\end{aligned}\right\}. \quad (8)$$

Accordingly, the *d*-*q* axes equivalent circuit is reconstructed as shown in Fig. 5. Then, the *d*-axis impedance is derived as

$$\dot{Z}_d^{AC} = R + \frac{R_i(\omega_e L)^2}{R_i^2+(\omega_e L)^2} + j\frac{R_i^2\omega_e L}{R_i^2+(\omega_e L)^2} \quad (9)$$

where ω_e is the applied voltage angular frequency. The following relation [3]:

$$\left(\frac{\omega_e L}{R_i}\right)^2 \ll 1 \quad (10)$$

simplifies the impedance as

$$\dot{Z}_d^{AC} = R + \frac{(\omega_e L)^2}{R_i} + j\omega_e L. \tag{11}$$

Since $\dot{Z}_d^{AC} = \dot{V}_d/\dot{I}_d$, the relationship between the applied voltage and line current is derived as

$$\dot{V}_{AC} = \frac{3}{2}\dot{Z}_d^{AC}\dot{I}_{AC}. \tag{12}$$

Then, the apparent power is expressed as

$$\dot{S}_{AC} = \frac{3}{2}\left(R + \frac{\omega_e^2 L^2}{R_i}\right)I_{AC}^2 + j\frac{3}{2}\omega_e L I_{AC}^2 \tag{13}$$

where the first and second terms in the right-hand side corresponds to the active power P_{AC} and reactive power Q_{AC}, respectively. Based on the the second term in (13), the armature inductance is identified as

$$L = \frac{2}{3}\frac{Q_{AC}}{\omega_e I_{AC}^2}. \tag{14}$$

Similarly, the iron loss resistance is identified from the first term in (13) as

$$R_i = \frac{(\omega_e L)^2}{\frac{2}{3}\frac{P_{AC}}{I_{AC}^2} - R}. \tag{15}$$

C. Synchronous Drive Test

The synchronous drive test topology is shown in Fig. 6. The geometry is normal for the three phase ac machines. When a three phase voltage is applied, the SPMSM synchronously rotates with applied angular frequency ($\omega_r = \omega_e$). In steady state condition, the d-q axes equivalent circuit is reconstructed as shown in Fig. 7. Then, (2) is rearranged as

$$\left.\begin{aligned} \Psi_d &= Li_d + K_e + \frac{\omega_e L}{R_i}Li_q \\ \Psi_q &= Li_q - \frac{\omega_e L}{R_i}(Li_d + K_e) \end{aligned}\right\}. \tag{16}$$

In steady state condition ($p = 0$), substituting (16) into (1) gives the voltage equation expressed in the form:

$$\begin{bmatrix} v_d \\ v_q \end{bmatrix} = \begin{bmatrix} R+\frac{(\omega_e L)^2}{R_i} & -\omega_e L \\ \omega_e L & R+\frac{(\omega_e L)^2}{R_i} \end{bmatrix}\begin{bmatrix} i_d \\ i_q \end{bmatrix} + \omega_e K_e \begin{bmatrix} \frac{\omega_e L}{Ri} \\ 1 \end{bmatrix}. \tag{17}$$

Since the impedance matrix in the first term is constant as long as the applied angular frequency is constant, the terminal voltage is proportion to the line current. Especially, when the line current is zero ($i_d = i_q = 0$), the terminal voltage is equal to the electromotive force as

$$\begin{bmatrix} v_d \\ v_q \end{bmatrix} = \omega_e K_e \begin{bmatrix} \frac{\omega_e L}{Ri} \\ 1 \end{bmatrix}. \tag{18}$$

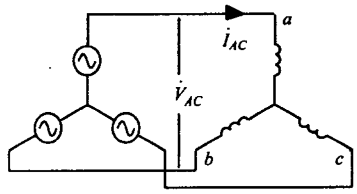

Fig. 6. Synchronous drive test topology.

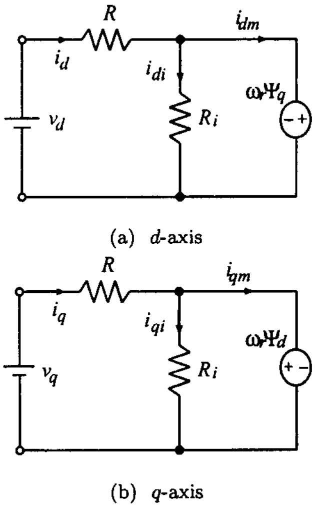

Fig. 7. d-q axes equivalent circuit under synchronous drive test.

Accordingly, the emf constant K_e is identified as

$$K_e = \frac{V_{AC}}{\omega_e} \tag{19}$$

where $V_{AC}(= \sqrt{v_d^2 + v_q^2})$ is the RMS of the terminal voltage. It takes notice that (10) is applied to the derivation of (19).

D. Current Control

In order to implement the self-commissioning strategy with inverter drive system, the phase current should be appropriately commutated according to the each test. To do this, the synchronous d-q axes current controller shown in Fig. 8 is constructed in this paper. For instance, the d-q axes current commands (i_d^*, i_q^*) are set to (5), the dc test is realized.

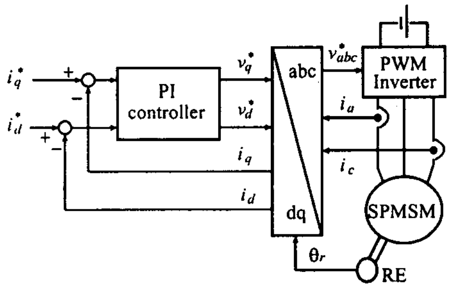

Fig. 8. Current control system.

E. Computation of Current, Voltage, and Power

In general, current sensors are installed in the inverter. Then, the instantaneous current information is easily available from the current sensor. However, the purchase of the instantaneous voltage information is difficult because the inverter output voltage is pulse wave form. For this reason, the voltage command of the inverter is substituted for the instantaneous voltage information. The dc current I_{DC}, dc voltage V_{DC}, RMS of ac current I_{AC}, RMS of ac voltage V_{AC}, active power P_{AC}, and reactive power Q_{AC} are computed with using the instantaneous current and voltage command informations as follows:

$$I_{DC} = \frac{1}{N}\sum_{k=1}^{N} i_{DC}(k) \tag{20}$$

$$V_{DC} = \frac{1}{N}\sum_{k=1}^{N} v_{DC}^{*}(k) \tag{21}$$

$$I_{AC} = \sqrt{\frac{1}{N}\sum_{k=1}^{N} i_{AC}(k)^2} \tag{22}$$

$$V_{AC} = \sqrt{\frac{1}{N}\sum_{k=1}^{N} v_{AC}^{*}(k)^2} \tag{23}$$

$$P_{AC} = \frac{1}{N}\sum_{k=1}^{N} i_{AC}(k)v_{AC}^{*}(k) \tag{24}$$

$$Q_{AC} = \sqrt{(V_{AC} * I_{AC})^2 - P_{AC}^2} \tag{25}$$

where $i_{DC}(k)$, $i_{AC}(k)$ are the detected currents at instant k, $v_{DC}^{*}(k)$, $v_{AC}^{*}(k)$ are the voltage commands at instant k, and N is the number of data during a period.

F. Influence of Switching Device Nonlinearity

The difference between the voltage command and actual voltage is essentially inevitable because the switching device of inverter has nonlinear characteristics due to the dead time and voltage drop. To compensate the influence of the voltage error on the computation of (21), (23), and (24), the voltage errors have been measured in advance. Figs. 9 to 12 show the differences between the voltage command and actual voltage detected with the digital power meter (DPM) for each test and the difference between the calculated active power and the actual one with DPM. These characteristics are utilized in the correction of the voltage command.

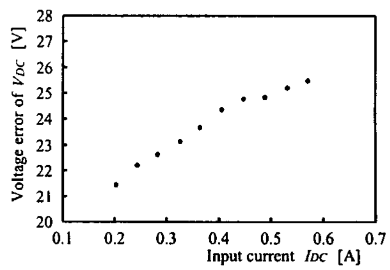

Fig. 9. Voltage error for dc test.

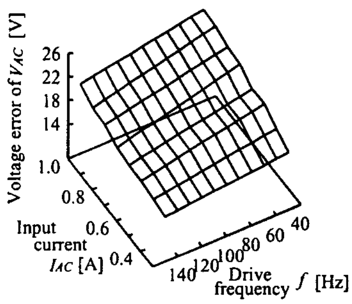

Fig. 10. Voltage error for single-phase ac test.

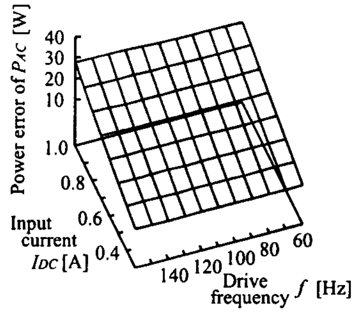

Fig. 11. Power error for single-phase ac test.

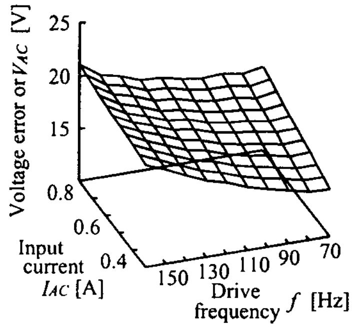

Fig. 12. Voltage error for synchronous test.

IV. Identification Results

To realize the dc test, single-phase ac test, and synchronous drive test, the current control system in Fig. 8 is incorporated into the ordinary inverter drive system. Table 1 shows the specification of the tested SPMSM.

A. DC Test

Fig. 13 shows the current control result for dc test. It can be confirmed from this figure that the line current is dc quantity. The identification result of the armature resistance R with using (6) is shown in Table 2. It almost agrees with the measured one with DPM.

B. Single-Phase AC Test

Fig. 14 shows the current control result for the single-phase ac test. It can be confirmed that the line current

Table 1. Specifications of tested SPMSM.

rated power	30 W
rated current	3.0 A
rated speed	1500 rpm (50π rad/s)
rated torque	0.19 N·m
number of pole pairs	8

Table 2. Self-commissioning results.

Parameter	SC	DPM	Error
R [Ω]	7.86	7.66	2.6%
L [H]	0.024	0.022	8.0%
R_i [Ω]	180	172	4.4%
K_e [V·s/rad]	0.049	0.047	4.3%

wave form is sinusoidal. The identification results of the armature inductance L with using (14) and the iron loss resistance R_i with using (15) for various applied frequency are shown in Figs. 15 and 16, respectively.

It follows from Fig. 15 that the armature inductance identified by the proposed self-commissioning strategy agrees well with the measured one with DPM. The obtained armature inductance increases with decreasing driving frequency because the ratio of the harmonic RMS increases in low frequency. The numerical results at 150Hz are listed in Table 2.

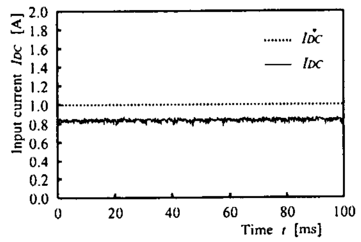

Fig. 13. Control result of dc current.

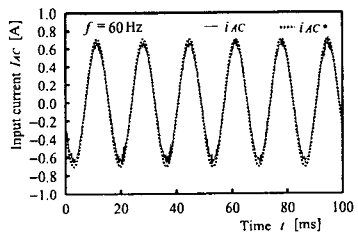

Fig. 14. Control result of single-phase ac current.

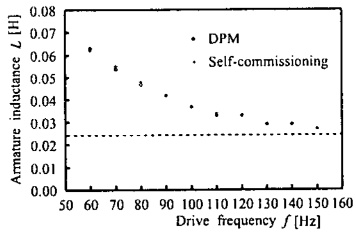

Fig. 15. Armature inductance.

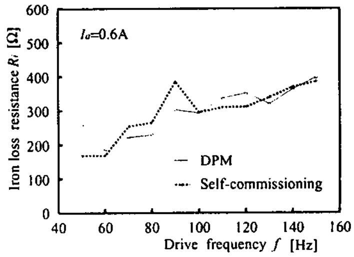

Fig. 16. Iron loss resistance.

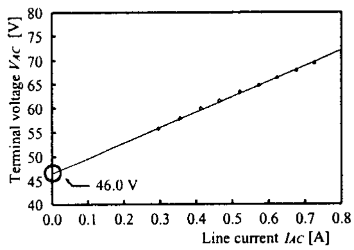

Fig. 17. Terminal voltage vs. line current under constant speed.

It follows from Fig. 16 that the iron loss resistance identified by the proposed strategy almost agrees with the measure one with DPM. However, the tested SPMSM is a small machine, that is, the iron loss is comparatively small. Then, either the identified and measured iron loss resistances are scattering. The numerical results at 60Hz are listed in Table 2.

C. Synchronous drive test

Fig. 17 shows the terminal voltage versus line current for the synchronous drive test at $\omega_r = 300\pi$ rad/s (f =150Hz). Since the characteristic is linear, the terminal voltage when the line current is zero, *i.e.*, electromotive force is easily estimated. The identification result of the emf constant K_e with using (19) is listed in Table 2. The identified emf constant agrees well with the measured one by the no-load generating test.

V. Conclusions

This paper proposes the self-commissioning for SPMSM. The dc test, single-phase ac test, and synchronous drive test are executed based on the synchronous d-q axis current controller incorporated in the ordinary inverter drive system. The automatic identification parameters almost agree with the measurement one by the manual operations.

References

[1] Y.-N. Lin and C.-L. Chen, "Automatic IM parameter measurement under sensorless field-oriented control," *IEEE Trans. Ind. Electron.*, vol. 46, no. 1, pp. 111-118, Feb., 1999.

[2] Y.-S. Lai, J.-C. Lin, and J. J. Wang, "Direct torque control induction motor drives with self-commissioning based on Taguchi methodology," *IEEE Trans. Power Electron.*, vol. 15, no. 6, pp. 1065-1071, Nov., 2000.

[3] N. Urasaki, T. Senjyu, and K. Uezato, "An accurate modeling for permanent magnet synchronous motor drives," in *Proc. APEC 2000*, New Orleans, pp. 387-392, 2000.